Design of a Triple-Band Patch Antenna for WLAN and C-band Applications

Ngozi Peggy Udeze, Akaa Agbaeze Eteng

Abstract— This paper discusses the design of a triple-band patch antenna. The employed approach first establishes patch sizes for the uppermost and lowest operating frequencies. Integrating both patches on a single substrate layer creates a single radiating patch with an inverted U-slot. A recessed transmission line is merged with this radiating patch to introduce a third operating frequency between the earlier established two frequencies. By a proper adjustment of antenna geometrical parameters, three operating frequencies are thus realized – 2.4 GHz, 4 GHz, and 5 GHz. Simulation results show moderate realized antenna gain levels of 4.9 dBi – 6.4 dBi at the operating frequencies. The proposed design has a potential to meet the need of current and imminent multiband wireless applications requiring support for WLAN and C-band operations.

Index Terms— Inverted U-slot, operating frequency, patch antenna, reflection coefficient, triple-band,

1 Introduction

PATCH antennas are popular as a consequence of their compact sizes, ease of production, and low-complexity [1]. These features, among others, have made them very attractive for integration into the RF frontends of devices requiring planar antennas.

It has become commonplace in contemporary communication systems for transceivers to support multiple communication services at different frequencies. This necessitates the deployment of antennas able to function at multiple frequencies. Consequently, multiband antennas have received considerable research and development interest in the past few years.

Several methods have been proposed to enable multiband functioning in patch antennas, such as incorporating slits and stubs [2], employing split-ring resonators [3], or using defected ground planes [4]. Of special interest is the use of U-slots [5] [6] [7] [8] [9], which leads to antennas with relatively large impedance bandwidths [7].

Generally, n operating frequencies can be obtained by loading n – 1 U-slots on the radiating patch. The isolation between the resonance frequency depends on the spacing between the etched slots [8] [6]. In applications where three bands or more are required within a relatively small range of frequencies, fabrication tolerances between the multiple U-slots may lead to a loss of the isolation between bands. The approach employed in this design study is to maintain the low-complexity of a U-slot design for a triple-band antenna, however, with the advantage of using only one U-slot. This U-slot is used to realize two frequency bands – the upper and lower frequencies. The third frequency is realized between these two frequency extremes by introducing a recessed transmission line on the same side as the radiating patch. The realized antenna is excited using a coplanar waveguide (CPW) feed behind the antenna. By optimizing the patch antenna size, the U-slot size, and the lengths of the transmission line recess and CPW feed, triple-band operation at the required frequencies is obtained.

This paper is organized as follows. First, the antenna design is presented. The method for obtaining the antenna size, and the U-slot layout is described. Initial dimensions for the RF feed and transmission line recess are similarly presented. Thereafter, simulation results based on an optimized geometry of the antenna are discussed.

2 Antenna Design

The initial antenna design is based on the transmission line model [1], which provides an analytical means to determine the size of the radiating patch. The width W of the radiating patch is determined using

$$W = \frac{C}{2f_r}\sqrt{\frac{2}{\epsilon_r+1}}, \quad (1)$$

where C is the free-space velocity of light, f_r is the desired resonance frequency, and ϵ_r is the relative permittivity of the chosen substrate material. Similarly, the length of the patch is determined by

$$L = \frac{C}{2f_r\sqrt{\epsilon_{reff}}} - 2\Delta L, \quad (2)$$

where ϵ_{reff} denotes the effective relative permittivity, and ΔL, a normalized extension in electrical length of the patch due to fringing effects. For a substrate thickness h, the effective relative permittivity can be calculated using

$$\epsilon_{reff} = \frac{\epsilon_r+1}{2} + \frac{\epsilon_r-1}{2}\left(1 + 12\frac{h}{W}\right)^{-0.5}. \quad (3)$$

An approximation for the normalized length extension ΔL is

- *Ngozi Peggy Udeze is studying at the the Department of Electrical/Electronic Engineering, University of Port-Harcourt, Port-Harcourt, Nigeria. Email: udezepeggy@yahoo.com*
- *Akaa Agbaeze Eteng is of the Department of Electrical/Electronic Engineering, University of Port-Harcourt, Port-Harcourt, Nigeria. Email: akaa.eteng@uniport.edu.ng*

$$\Delta L = 0.412h\frac{\epsilon_{reff}+0.3\left(\frac{W}{h}+0.264\right)}{\epsilon_{reff}-0.258\left(\frac{W}{h}+0.8\right)}. \quad (4)$$

Using equations (1) - (4), initial radiating patch sizes for operation at 2.4 GHz and 5 GHz are realized, for an FR-4 substrate having a relative permittivity ϵ_r = 4.7. Having obtained the initial antenna dimensions, the approach is to embed the smaller-sized 5 GHz patch within the 2.4 GHz patch, as inspired by [8], thereby realizing a single patch with an inverted U-slot. To obtain a third operating frequency between 2.4 GHz and 5 GHz, a recessed transmission line with length y_0 is integrated into the radiating patch. The antenna is energized using a shorted coplanar wave guide (CPW) feed of length y etched behind the antenna.

The resulting antenna structure is shown in Fig. 1, while Table 1 lists the antenna parameters. The subscripts "1" and "2" are used to denote dimensions for the 2.4 GHz and 5 GHz patches, respectively. In the initial antenna iteration, the dimensions for y_0, y , f, r, and g , as listed in Table 1 are arbitrary. While the g dimension was chosen with consideration for fabrication tolerances, the choice for r was predicated on the need for a current path to the L_1 patch edges.

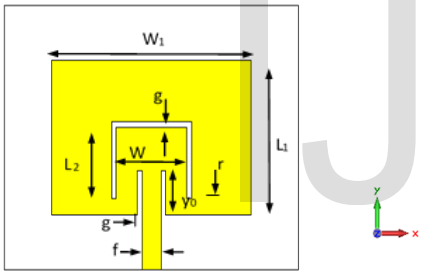

(a) Front view

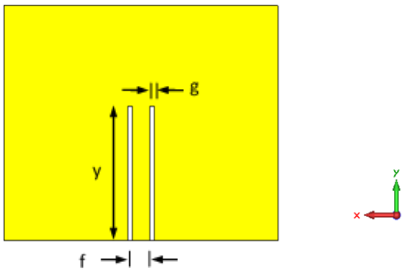

(b) Back view

Fig. 1. Antenna geometry

TABLE 1
Initial Antenna Parameters

Parameter	Dimension (mm)
W_1	36.27
L_1	27.91
y_0	9.39
W_2	17.77
L_2	13.33
y	30
f	4
r	4
g	1

3 Results and Discussion

Electromagnetic (EM) simulations of the antenna structure were performed using a full-wave EM solver, CST Microwave Studio ©. A parametric study was conducted to ascertain the impact of the length y_0 of the recessed transmission line, and the length y of the CPW feed on the reflection coefficient as shown in Figs. 2 and 3, respectively. Fig. 2 was obtained by varying the dimension y_0, with y held constant; while Fig 3 was obtained with y_0 varying, with y held constant.

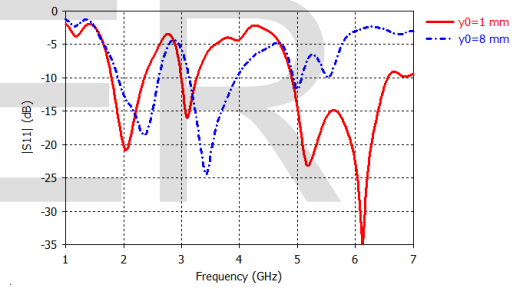

Fig. 2 Parametric study of length y_0 of transmission line recess

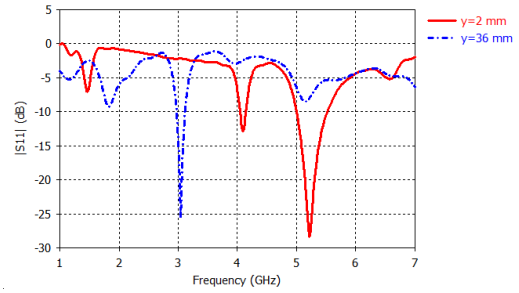

Fig. 3 Parametric study of length y of CPW feed

From Fig. 2, it can be observed that the inclusion of a recessed transmission line causes the appearance of multiple resonant frequencies within the observed range. With a recess length y_0 of 1 mm, four resonances modes are observed – at 2 GHz, 3.1 GHz, at 5.2 GHz, and at 6.5 GHz. Increasing y_0 to 8 mm leads to a modification of the observed resonance frequencies, which now centre at 2.4 GHz, 3.4 GHz, 5 GHz, and 5.5 GHz.

Also, it can be seen that increasing y_0 leads to the second resonance being deeper than others. Similarly, it can also be observed from Fig. 3 that increasing the length y causes a downward shift in the frequency at which the deepest resonance is obtained. Furthermore, it can be observed that with an increase in y, the second resonance position becomes the deepest and most clearly defined. In summary, Figs. 2 and 3 reveal the existence of multiple modes from which three resonance frequencies can be harnessed by an optimization of patch size dimensionan, as well as the lengths y_0 and y. Consequently, the dimensions W_1, W_2, L_1, L_2, y_0, y and r are optimized using the full-wave EM solver to obtain reflection coefficient magnitudes ($|S_{11}|$) less than – 10 dB at the specified resonance frequencies of 2.4 GHz, 4 GHz, and 5 GHz. The optimized values are shown in Table 2.

TABLE 2
Optimized Antenna Parameters

Parameter	Dimension (mm)
W_1	40.61
L_1	27.48
y_0	6.79
W_2	13.22
L_2	11.00
r	4.88
y	27.93

The reflection coefficient for the realized antenna is shown in Fig 4. From the Figure, $|S_{11}|$ values of less than -10 dB were achieved at 2.4 GHz, 4 GHz and 5 GHz, which implies resonance at these frequencies. The impedance bandwidths are 17.5%, 31.25%, and 11%, at 2.4 GHz, 4 GHz, and 5 GHz, respectively.

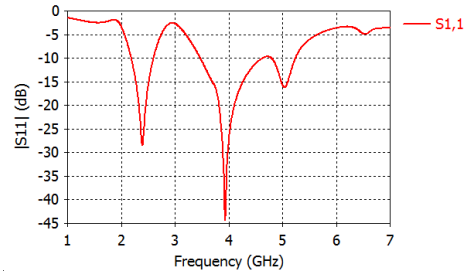

Fig. 4. Reflection coefficient of realized antenna

The current distribution on the radiating patch at the three resonant frequencies can be observed from Fig. 5. At 2.4 GHz, the current is densely distributed over almost all the patch. At 4 GHz, however, the current is strongly concentrated at the transmission line recess, while the U-slot edges, dimensioned L_2 , also have impact on the radiation performance. Finally, at 5 GHz, surface current is more localized along the L_2 dimension, and towards the patch edges. These results are a pointer to the impact of the various patch dimensions on the realization of resonance at the three specified frequencies.

The 3D radiation patterns obtained at the resonant frequencies are shown in Fig. 6. These plots show that the antenna main beam is directed at $\theta = 0^0$ in the azimuth for all resonant frequencies, while the elevation angle deviates from $\varphi = 0^0$, at 4 GHz and 5 GHz. The realized gains are 6.4 dBi, 6.1 dBi, and 4.9 dBi, at 2.4 GHz, 4 GHz, and 5 GHz, respectively.

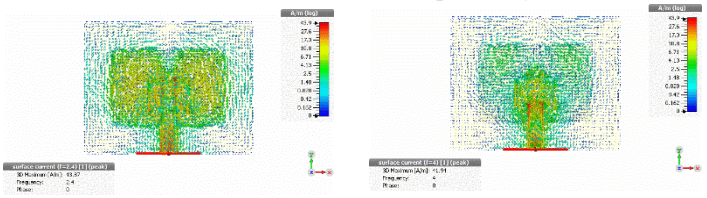

(a) 2.45 GHz (b) 4 GHz

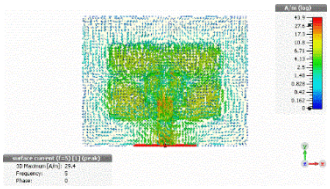

(c) 5 GHz

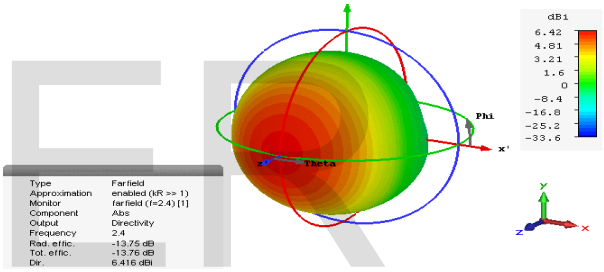

(a) 2.4 GHz

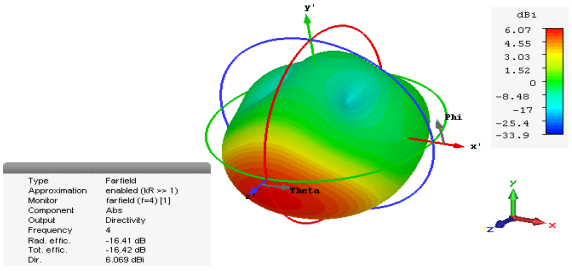

(b) 4 GHz

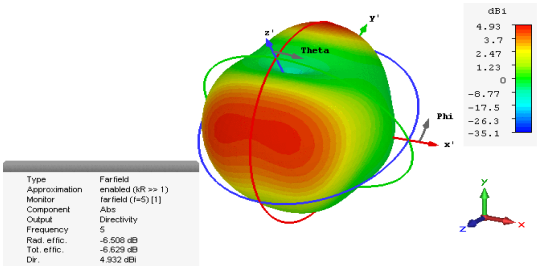

(c) 5 GHz

Fig. 6 Antenna 3D radiation patterns

Fig. 7 shows the H-plane antenna radiation pattern at the three resonance frequencies. For all three resonance frequencies, there is an acceptable level of discrimination between the antenna cross- and co-polarization patterns. At 2.45 GHz there is about 18 dBi difference in the magnitude of the co- and cross-polarization mainlobe patterns. There is a lower level of discrimination between co-and cross-polarization mainlobe patterns at 4 GHz, with a difference of 5.5 dBi observed. However, this value improves to 7.8 dBi at 5 GHz.

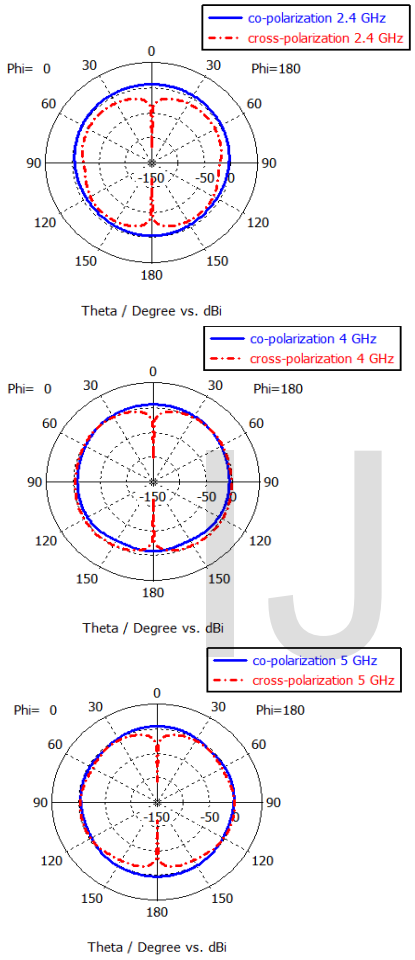

Fig 7. H-plane antenna radiation patterns for 2.4 GHz, 4 GHz, and 5 GHz (top-to-bottom)

For the E-plane radiation plot, the discrimination between co-and cross-polarization patterns is even more pronounced, as observed from Fig. 8. More than 100 dBi difference between co- and cross-polarization mainlobe magnitudes is observed at the three resonance frequencies.

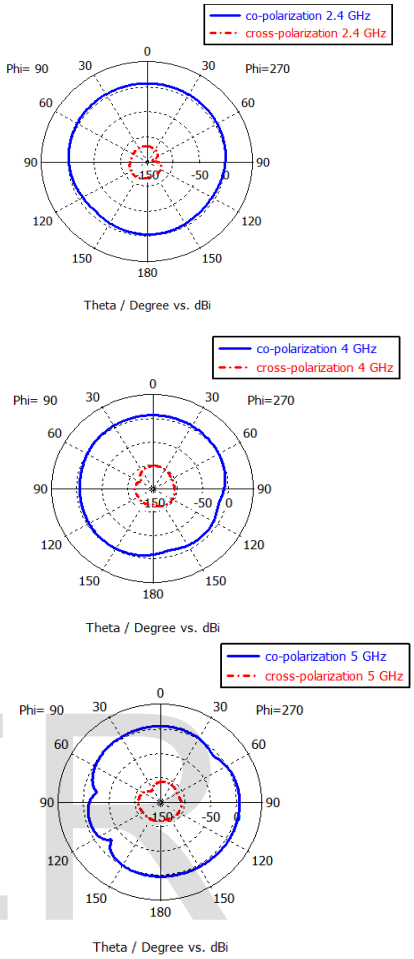

Fig 8. E-plane antenna radiation patterns 2.4 GHz, 4 GHz, and 5 GHz (top-to-bottom).

CONCLUSION

This paper has presented a design study of a triple-band patch antenna, with operational frequencies of 2.4 GHz, 4 GHz, and 5 GHz. The procedure for realizing these three operational frequencies has been discussed. Simulation results indicate impedance bandwidths of 17.5%, 31.25%, and 11%, at 2.4 GHz, 4 GHz, and 5 GHz, respectively. In addition, moderate gains in the range of 6.4 dBi – 4.9 dBi were achieved at the three frequency bands. The results show the potential for utilizing the proposed triple-band antenna design in WLAN and C-band applications.

REFERENCES

[1] C. A. Balanis, *Antenna Theory: Analysis and Design*, 3rd ed. John Wiley & Sons, 2005.

[2] S. Mathew, M. Ameen, M. P. Jayakrishnan, P. Mohanan, and K. Vasudevan, "Compact dual polarised v slit, stub and slot

embedded circular patch antenna for UMTS/WiMAX/WLAN applications," *Electron. Lett.*, vol. 52, no. 17, pp. 1425–1426, 2016.

[3] W. Ali, E. Hamad, M. Bassiuny, and M. Hamdallah, "Complementary split ring resonator based triple band microstrip antenna for WLAN/WiMAX applications," *Radioengineering*, vol. 26, no. 1, pp. 78–84, 2017.

[4] M. Z. M. Nor, S. K. a. Rahim, M. I. Sabran, and M. S. a. Rani, "Slotted dual band directive antenna with defected ground plane structure," *2013 Asia-Pacific Microw. Conf. Proc.*, pp. 432–434, Nov. 2013.

[5] W. C. Mok, S. H. Wong, K. M. Luk, and K. F. Lee, "Single-Layer single-patch dual-band and triple-band patch antennas," *IEEE Trans. Antennas Propag.*, vol. 61, no. 8, pp. 4341–4344, 2013.

[6] K. F. Lee, K. M. Luk, K. M. Mak, and S. L. S. Yang, "On the use of U-slots in the design of dual-and triple-band patch antennas," *IEEE Antennas Propag. Mag.*, vol. 53, no. 3, pp. 60–74, 2011.

[7] J. J. Borchardt and T. C. Lapointe, "U-Slot Patch Antenna Principle and Design Methodology Using Characteristic Mode Analysis and Coupled Mode Theory," *IEEE Access*, vol. 7, pp. 109375–109385, 2019.

[8] A. Boukarkar, X. Q. Lin, Y. Jiang, and Y. Q. Yu, "Miniaturized Single-Feed Multiband Patch Antennas," *IEEE Trans. Antennas Propag.*, vol. 65, no. 2, pp. 850–854, 2017.

[9] A. Boukarkar, X. Q. Lin, J. W. Yu, P. Mei, Y. Jiang, and Y. Q. Yu, "A Highly Integrated Independently Tunable Triple-Band Patch Antenna," *IEEE Antennas Wirel. Propag. Lett.*, vol. 16, no. c, pp. 2216–2219, 2017.